mRNA-binding protein tristetraprolin is essential for cardiac response to iron deficiency by regulating mitochondrial function

Tatsuya Sato[a,1], Hsiang-Chun Chang[a,1], Marina Bayeva[a], Jason S. Shapiro[a], Lucia Ramos-Alonso[b], Hidemichi Kouzu[a], Xinghang Jiang[a], Ting Liu[a], Sumeyye Yar[a], Konrad T. Sawicki[a], Chunlei Chen[a], María Teresa Martínez-Pastor[c], Deborah J. Stumpo[d], Paul T. Schumacker[e], Perry J. Blackshear[d], Issam Ben-Sahra[f], Sergi Puig[b], and Hossein Ardehali[a,2]

[a]Feinberg Cardiovascular Research Institute, Feinberg School of Medicine, Northwestern University, Chicago, IL 60611; [b]Departamento de Biotecnología, Instituto de Agroquímica y Tecnología de Alimentos, Consejo Superior de Investigaciones Científicas, 46980 Paterna, Valencia, Spain; [c]Departamento de Bioquímica y Biología Molecular, Universitat de València, 46100 Burjassot, Valencia, Spain; [d]Signal Transduction Laboratory, National Institute of Environmental Health Sciences, Research Triangle Park, NC 27709; [e]Department of Pediatrics, Feinberg School of Medicine, Northwestern University, Chicago, IL 60611; and [f]Department of Biochemistry and Molecular Genetics, Feinberg School of Medicine, Northwestern University, Chicago, IL 60611

Edited by J. G. Seidman, Harvard Medical School, Boston, MA, and approved May 23, 2018 (received for review March 23, 2018)

Cells respond to iron deficiency by activating iron-regulatory proteins to increase cellular iron uptake and availability. However, it is not clear how cells adapt to conditions when cellular iron uptake does not fully match iron demand. Here, we show that the mRNA-binding protein tristetraprolin (TTP) is induced by iron deficiency and degrades mRNAs of mitochondrial Fe/S-cluster-containing proteins, specifically *Ndufs1* in complex I and *Uqcrfs1* in complex III, to match the decrease in Fe/S-cluster availability. In the absence of TTP, *Uqcrfs1* levels are not decreased in iron deficiency, resulting in nonfunctional complex III, electron leakage, and oxidative damage. Mice with deletion of *Ttp* display cardiac dysfunction with iron deficiency, demonstrating that TTP is necessary for maintaining cardiac function in the setting of low cellular iron. Altogether, our results describe a pathway that is activated in iron deficiency to regulate mitochondrial function to match the availability of Fe/S clusters.

iron | mRNA-binding protein | cardiomyopathy | mitochondrial complex | reactive oxygen species

Iron deficiency is the most common nutrient deficiency in the world (1). In response to iron deficiency, mammalian cells activate two iron regulatory proteins (IRPs), IRP1 and IRP2 (2, 3). These proteins bind to iron-response elements in the 3′ UTR of transferrin receptor 1 (*Tfrc*) mRNA, causing stabilization of *Tfrc* mRNA and an increase in iron uptake into the cell. Conversely, IRP1/2 also bind to the 5′ UTR of ferroportin-1 (*Fpn1*, also known as *Slc40a1*) and ferritin heavy-chain and light-chain (*Fth1* and *Ftl*) mRNAs, causing decreased translation of these mRNAs, which results in reduced iron export and increased cellular iron availability, respectively (4–7). Thus, the activation of the IRP pathway leads to increased cellular iron acquisition. While the purpose of the IRP system is to restore cellular iron homeostasis, prolonged and/or severe iron deficiency could outpace the ability of the IRP system to normalize cellular iron levels. We recently discovered a parallel pathway involving the mRNA-binding protein tristetraprolin (TTP, also known as ZFP36) that is activated when cellular iron levels are severely decreased (8). TTP is a tandem zinc-finger (TZF) protein that binds to the AU-rich elements (AREs) in the 3′ UTR of mRNA molecules and promotes their degradation (9). The pathway involving TTP appears to conserve cellular iron in lieu of further uptake and protects against cell death (i.e., iron conservation pathway) (8, 10). However, the precise mechanism by which TTP up-regulation conserves iron and promotes cell survival in iron deficiency is not clear.

In mammalian cells, mitochondrial oxidative metabolism is one of the major consumers of iron, with Fe/S clusters and heme groups found in multiple subunits of complexes I–IV of the electron transport chain (ETC) (11). However, energy production by oxidative phosphorylation in mitochondria is nonessential for survival, at least in the short term, as demonstrated by a switch to anaerobic respiration and heavy reliance on glycolysis in muscle during vigorous exercise, when oxygen demand outmatches its supply (12). Thus, in states of limited iron availability, continuous production of iron-containing ETC subunits for use in oxidative phosphorylation can divert iron from more essential pathways, turning this pathway into an iron "sink" and jeopardizing cell viability. In this scenario, preferentially shutting down mitochondrial oxidative phosphorylation may prevent excessive iron utilization by the mitochondria, freeing up the limited iron supply for use in other cellular functions and promoting survival. Moreover, lack of sufficient iron can result in accumulation of the nonfunctional apo form of ETC components, which can subsequently lead to formation of nonfunctional ETC complexes, leakage of electrons, and generation of oxidative radicals and cellular damage. The molecular safeguard against these two scenarios has not been identified.

Significance

Iron deficiency is the most common nutrient deficiency, yet cardiomyopathy rarely develops in these patients. We solved this paradox and identified a protective mechanism involving the mRNA-binding protein tristetraprolin (TTP), which adjusts mitochondrial function in response to iron deficiency. Mice lacking TTP in their hearts were phenotypically normal at baseline but developed spontaneous cardiomyopathy under iron deficiency and exhibited increased reactive oxygen species (ROS)-mediated damage in their hearts. We further demonstrate that down-regulation of specific iron-containing mitochondrial complexes by TTP is the mechanism preventing the formation of dysfunctional mitochondria, subsequent ROS production, and cellular damage. In summary, we show that activation of TTP is part of a required pathway protecting critical organ function when iron becomes scarce.

Author contributions: T.S., H.-C.C., M.B., and H.A. designed research; T.S., H.-C.C., J.S.S., L.R.-A., H.K., X.J., T.L., S.Y., C.C., M.T.M.-P., and S.P. performed research; D.J.S., P.J.B., and I.B.-S. contributed new reagents/analytic tools; T.S., H.-C.C., J.S.S., and P.T.S. analyzed data; and T.S., H.-C.C., M.B., J.S.S., K.T.S., and H.A. wrote the paper.

The authors declare no conflict of interest.

This article is a PNAS Direct Submission.

[1]T.S. and H.-C.C. contributed equally to this work.

[2]To whom correspondence should be addressed. Email: h-ardehali@northwestern.edu.

This article contains supporting information online at www.pnas.org/lookup/suppl/doi:10.1073/pnas.1804701115/-/DCSupplemental.

Published online June 18, 2018.

Here, we demonstrate that TTP degrades mRNAs of select mitochondrial Fe/S-containing proteins to parallel the drop in iron levels in states of deficiency. Interruption of this TTP-dependent pathway in iron deficiency leads to the formation of apo-UQCRFS1, a component of complex III, which results in reactive oxygen species (ROS) production and cell death. In addition, we demonstrate that in iron deficiency *Ttp* KO mice display cardiomyopathy (CM) and cellular damage, while control mice maintain cardiac function, implicating the necessity for TTP up-regulation in cellular physiology in the setting of iron deficiency. Overall, our results provide a link between mitochondrial function and availability of cellular iron.

Results

TTP Regulates mRNAs of Key Mitochondrial Proteins. Mitochondria utilize a large number of Fe/S-cluster-containing proteins for oxidative phosphorylation, yet energy production by mitochondria is not essential for cell survival, at least in the short term. Thus, we hypothesized that cells can potentially respond to iron deficiency by suppressing the production of mitochondrial ETC and TCA-cycle components to prevent them from becoming an "Fe/S cluster sink," and that TTP is a key player in this process by posttranscriptionally regulating the levels of iron-containing ETC components. To identify the mitochondrial targets of TTP, we took an unbiased in silico approach and screened the mRNA transcripts of all genes in the ETC and TCA cycle for the presence of AREs. We also assessed whether those AREs are conserved across human, rat, and mouse species. Our analyses revealed several transcripts for mitochondrial proteins as potential targets of TTP (*SI Appendix*, Table S1). We then assessed the steady-state mRNA levels of these potential targets of TTP using WT and *Ttp* KO mouse embryonic fibroblasts (MEFs) in the presence and absence of iron chelation. Because TTP is induced with cellular iron deficiency to promote degradation of its target transcripts, we would expect the mRNA levels of TTP target genes to be decreased during iron chelation when TTP is present but remain elevated with TTP deletion. We used 2,2′-bipyridyl (BPD) as an iron chelator and confirmed that *Ttp* mRNA and protein levels increase with iron chelation in WT MEFs (Fig. 1*A* and *SI Appendix*, Fig. S1*A*), as described previously (8). Treatment of both WT and *Ttp* KO MEFs with BPD resulted in a significant decrease in total cellular nonheme iron (Fig. 1*B*), confirming the effectiveness of BPD in depleting cellular iron. Analysis of steady-state mRNA levels revealed the following in silico-predicted mRNAs to be decreased with iron chelation in WT MEFs but not in *Ttp* KO MEFs: TCA cycle: *Aco2*; complex I: *Ndufs1*, *Ndufaf4*, *Ndufaf6*; complex II: none; complex III: *Uqcrfs1*; complex IV: *Cox15*; complex V: *Atp5b* (Fig. 1 *C–I* and *SI Appendix*, Fig. S1*B*).

To confirm that these proteins are posttranscriptionally regulated by TTP in iron chelation, we performed mRNA decay studies on the potential TTP target transcripts after treatment with the RNA polymerase inhibitor actinomycin D in WT and *Ttp* KO MEFs. These studies revealed that only *Ndufs1*, *Ndufaf4* (complex I), *Uqcrfs1* (complex III), and *Aco2* (TCA cycle) display slower rates of decay in *Ttp* KO compared with WT MEFs (Fig. 2*A* and *SI Appendix*, Fig. S2).

We then assessed the protein levels of NDUFS1, NDUFAF4, UQCRFS1, and ACO2 in H9c2 cells treated with control or *Ttp* siRNA in the absence of iron chelation and 16 and 32 h after treatment with BPD. We first confirmed that iron chelation increased the protein levels of TTP in control H9c2 cells, but not in cells pretreated with *Ttp* siRNA (Fig. 2 *B* and *C*), and that BPD treatment reduced cellular, mitochondrial, and cytosolic iron levels (*SI Appendix*, Fig. S3 *A–D*). While protein levels of NDUFS1, UQCRFS1, and ACO2 were decreased with iron chelation in H9c2 cells treated with control siRNA, this response was either completely or partially reversed in cells treated with *Ttp* siRNA (Fig. 2 *B* and *D–F*). Among these proteins, UQCRFS1 levels displayed the most prominent decrease under iron deficiency in control siRNA-treated cells and remained unchanged in *Ttp* siRNA-treated cells, suggesting that the major target of TTP in this pathway may be UQCRFS1. However, NDUFAF4 showed a pattern that was not totally consistent with its regulation by TTP; although its decrease with iron chelation was attenuated with *Ttp* siRNA, NDUFAF4 protein levels decreased after *Ttp* knockdown (KD) at baseline (Fig. 2 *B* and *G*), suggesting that it is likely not a target of TTP. This observation, along with the fact that NDUFAF4 is not an Fe/S-containing protein, prompted us to focus the remaining studies on NDUFS1, UQCRFS1, and ACO2 (Fig. 2*B*).

To confirm our findings, we then assessed the effects of TTP overexpression on these proteins. Overexpression of WT human *TTP* (h*TTP*) in H9c2 cells was associated with significant reduction in the protein levels of NDUFS1, UQCRFS1, and

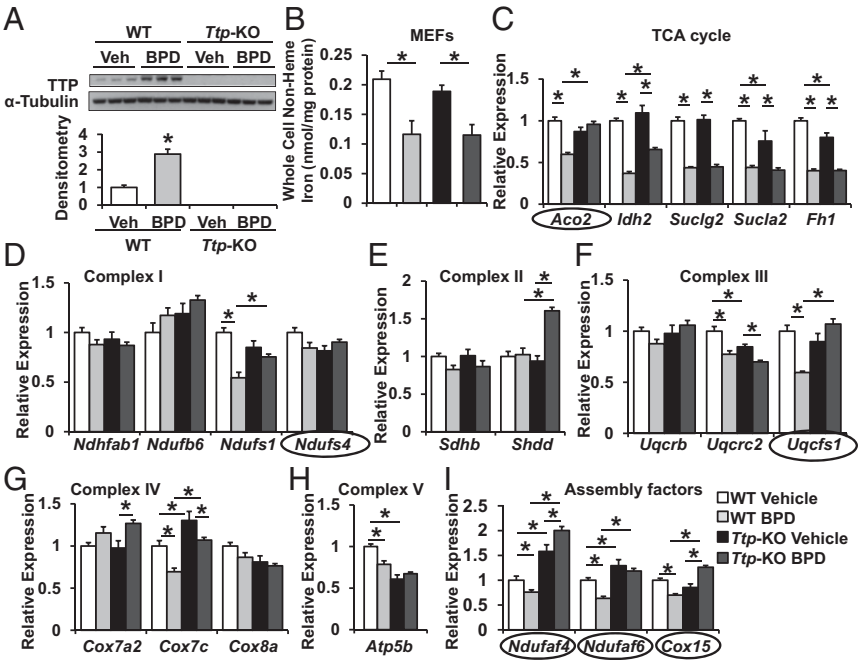

Fig. 1. TTP regulates the expression of mitochondrial proteins in response to iron deficiency. (*A* and *B*) TTP protein (*A*) and cellular nonheme iron (*B*) levels in WT and *Ttp* KO MEFs in response to 24-h treatment with 80 μM BPD. (*C–I*) Changes in mRNA levels of TCA cycle (*C*), complex I (*D*), complex II (*E*), complex III (*F*), complex IV (*G*), complex V (*H*), and assembly factor (*I*) proteins with AREs in their 3′ UTR in WT and *Ttp* KO MEFs in response to BPD. mRNAs that display a decrease with iron deficiency in WT MEFs but not in *Ttp* KO MEFs are circled. $n = 3$ for *A* and 6 for *B–I*. All graphs show mean ± SEM. *$P < 0.05$ by ANOVA with Tukey post hoc analysis. Veh, vehicle.

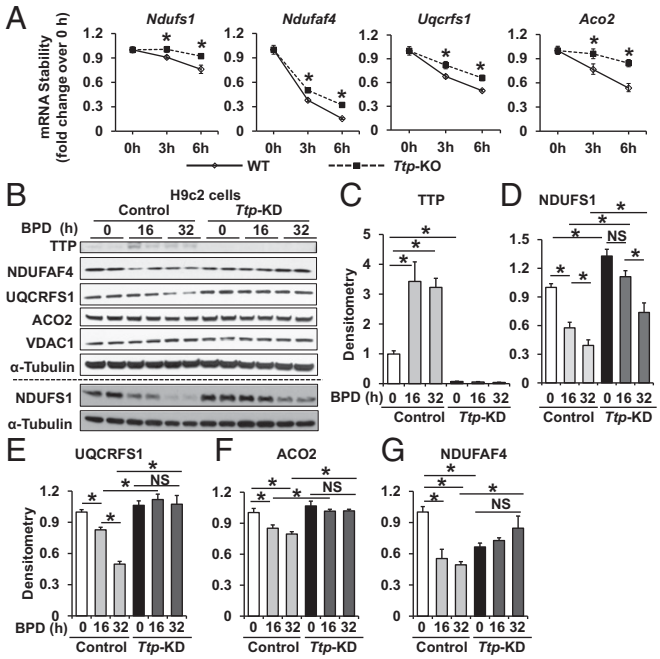

Fig. 2. *Aco2*, *Ndufs1*, and *Uqcrfs1* mRNA decay and protein levels are regulated by TTP. (*A*) mRNA stability of *Ndufs1*, *Ndufaf4*, *Uqcrfs1*, and *Aco2* in WT and *Ttp* KO MEFs treated with 7.5 μM actinomycin D. Samples were normalized to their respective RNA levels at time 0. $n = 6$ per time point. $^*P < 0.05$ by unpaired Student's *t* test. (*B–G*) Representative Western blot (*B*) and densitometry (*C–G*) of various proteins in H9c2 cells with indicated treatment. $n = 4$ per group, with *B* showing two representative samples. $^*P < 0.05$ by with ANOVA with Tukey post hoc analysis. All graphs show mean ± SEM. NS, not significant.

ACO2, but overexpression of nonfunctional TZF mutant *TTP* (C124R) failed to produce a similar effect (*SI Appendix*, Fig. S3 *E* and *F*). These results demonstrate that TTP induction is necessary for reductions in the protein levels of NDUFS1, UQCRFS1, and ACO2 in the setting of cellular iron depletion.

We then measured the abundance of these proteins in mice with global *Ttp* deletion in the presence and absence of iron deficiency. Because TNFα is a well-established target of TTP and global *Ttp* deletion leads to increased production of TNFα and systemic inflammation, we used mice with a background deletion of TNFα receptors-1 and -2 (*Tnfrsf1a* and *Tnfrsf1b*), referred to as $Tnfr1/2^{-/-}$, to examine the effects of iron deficiency independent of inflammation (13) (*SI Appendix*, Fig. S4 *A* and *B*). To induce iron deficiency, $Tnfr1/2^{-/-}$ (control) and $Tnfr1/2^{-/-}/Ttp^{-/-}$ mice were fed a regular or iron-deficient diet for 6 wk starting on postnatal day 21 (P21) (*SI Appendix*, Fig. S4*C*). $Tnfr1/2^{-/-}$ and $Tnfr1/2^{-/-}/Ttp^{-/-}$ mice fed an iron-deficient diet displayed a similar decrease in serum iron and serum transferrin iron saturation and an increase in unsaturated iron-binding capacity compared with mice of the same genotype fed a control diet, and there was no difference in these effects in male vs. female mice (*SI Appendix*, Fig. S4 *D–F* and Table S2). Furthermore, iron deficiency was associated with a decrease in hemoglobin (Hgb), hematocrit (HCT), and mean corpuscular volume, no change in white blood cell count, and an increase in platelet count (*SI Appendix*, Fig. S4 *G–K* and Table S2). There was a slight but significantly greater reduction in Hgb and HCT in $Tnfr1/2^{-/-}/Ttp^{-/-}$ than in $Tnfr1/2^{-/-}$ mice with iron deficiency (*SI Appendix*, Fig. S4 *G* and *H* and Table S2). Assessment of iron in the hearts of these mice showed a significant decrease in total, mitochondrial, and cytosolic nonheme iron in both $Tnfr1/2^{-/-}$ and $Tnfr1/2^{-/-}/Ttp^{-/-}$ murine hearts after iron deprivation (Fig. 3 *A–D*), suggesting that the diet-induced iron deficiency depletes iron not only in the circulation but also in the heart. There was no difference between $Tnfr1/2^{-/-}$ and $Tnfr1/2^{-/-}/Ttp^{-/-}$ mice in food intake, body weight (BW), or tibial length (TL) (*SI Appendix*, Fig. S4 *L–N*).

Consistent with decreased iron in the heart, TFRC protein levels were increased in both $Tnfr1/2^{-/-}$ and $Tnfr1/2^{-/-}/Ttp^{-/-}$ mice after iron deprivation, while TTP protein levels were also increased in $Tnfr1/2^{-/-}$ mice under iron deficiency (Fig. 3 *E–G*). Protein levels of NDUFS1, UQCRFS1, and ACO2 in the heart were decreased after treatment with iron-deficient diet in the control $Tnfr1/2^{-/-}$ mice, but these reductions were reversed in the $Tnfr1/2^{-/-}/Ttp^{-/-}$ mice (Fig. 3 *E* and *H*). The modest reduction in protein levels is likely due to the small increase in TTP protein levels under chronic iron deficiency. Nevertheless, these results further indicate that TTP is necessary for the change in the cardiac levels of NDUFS1, UQCRFS1, and ACO2 proteins in iron deficiency.

TTP Binds to *Ndufs1*, *Uqcrfs1*, and *Aco2* mRNAs Independent of Hypoxia-Inducible Factor and IRP Pathways. We then assessed whether TTP protein binds to *Ndufs1*, *Uqcrfs1*, and *Aco2* mRNAs using RNA coimmunoprecipitation studies. As shown in Fig. 4*A*, the mRNAs for these proteins displayed higher binding to TTP antibody compared with IgG. We also assessed whether IRPs play a role in the effects of iron chelation on NDUFS1, UQCRFS1, and ACO2. *Irp1* KD in *Irp2* KO MEFs was achieved using siRNA against *Irp1* (Fig. 4*B*). Iron deficiency in *Irp1* KD/*Irp2* KO cells led to increased TTP protein levels, as expected, and also led to decreased NDUFS1, UQCRFS1, and ACO2 protein levels, as predicted from increased TTP expression (Fig. 4 *C* and *D*). Together, these results suggest that TTP-mediated mRNA regulation of *Ndufs1*, *Uqcrfs1*, and *Aco2* in iron deficiency is independent of the IRP pathway.

Since iron deficiency activates the hypoxia-inducible factor (HIF) pathway (14, 15), we then conducted studies to ensure that the observed changes in the above targets are not explained by activation of the HIF pathway. To inactivate HIF-dependent gene expression, MEFs with genetic deletion of the Aryl Hydrocarbon Nuclear Receptor Translocator (*Arnt*, encoding an obligatory dimerization partner for HIF1α and HIF2α) were treated with BPD. *Arnt* KO MEFs exhibited reduced mRNA

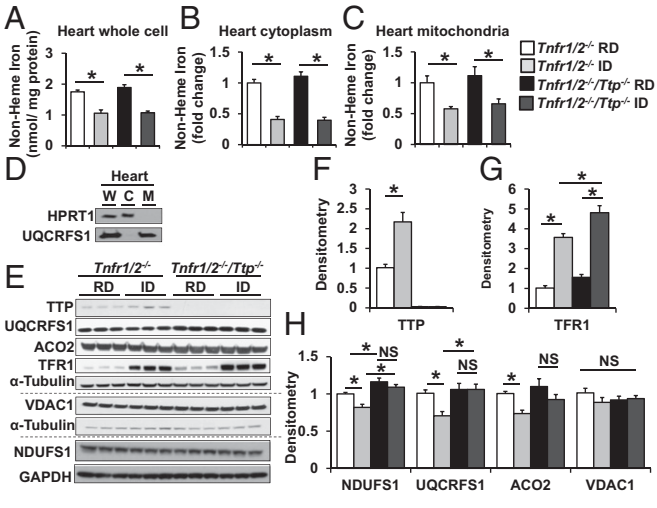

Fig. 3. Iron deficiency in mice increases TTP protein level and decreases NDUFS1, UQCRFS1, and ACO2 protein levels. (*A–C*) Nonheme iron in whole cell (*A*), cytoplasm (*B*), and mitochondria (*C*) of $Tnfr1/2^{-/-}$ and $Tnfr1/2^{-/-}/Ttp^{-/-}$ hearts with iron deficiency. (*D*) Western blot confirming the purity of mitochondrial isolation. (*E–H*) Western blot (*E*) and densitometry (*F–H*) of various proteins in hearts from $Tnfr1/2^{-/-}$ and $Tnfr1/2^{-/-}/Ttp^{-/-}$ mice receiving regular diet (RD) and iron-deficient diet (ID). All graphs show mean ± SEM. $^*P < 0.05$ by ANOVA with Tukey post hoc analysis. C, cytoplasm; M, mitochondria; W, whole cell. NS, not significant.

levels of *Ndufs1*, *Uqcrfs1*, and *Aco2* during iron chelation (Fig. 4*E*), similar to what we observed in WT MEFs under iron deficiency (Fig. 1 *C*, *D*, and *F*), indicating that the effects of iron chelation on the expression of these mRNAs were independent of HIF.

Although the mRNA levels of mitochondrial iron-containing proteins decreased with iron chelation, *Ttp* deletion at baseline (without iron deficiency) did not lead to an increase in their mRNA levels (Fig. 1 *C*–*G*). The lack of increase in the mRNA of these proteins in *Ttp* KO MEFs is likely due to the long-term adaption of these cells to chronic deletion of *Ttp*. To test this hypothesis, we measured steady-state mRNA levels of *Ndufs1*, *Uqcrfs1*, and *Aco2* in H9c2 rat cardiomyoblasts in the presence and absence of *Ttp* siRNA treatment to mimic acute reduction of TTP. Treatment with *Ttp* siRNA resulted in a significant decrease in TTP protein levels (*SI Appendix*, Fig. S5*A*), as well as increases in the steady-state mRNA levels and decreases in mRNA decay of *Ndufs1*, *Uqcrfs1*, and *Aco2* (*SI Appendix*, Fig. S5 *B* and *C*).

Yeast Homologs of TTP Regulate ETC and Aconitase mRNAs in Iron Deficiency. In response to iron deficiency, the budding yeast *Saccharomyces cerevisiae* expresses two TTP homologs known as *CTH1* and *CTH2*. Both yeast proteins bind to and promote the decay of many ARE-containing mRNAs that encode proteins involved in iron-consuming pathways, including mitochondrial respiration (16, 17). Previous work has demonstrated that TTP can functionally substitute for the Cth2 protein when expressed in yeast (8). Therefore, we assessed whether TTP can target and degrade mRNAs within the yeast ETC and TCA cycle. It should be noted that, unlike mammalian cells, other mechanisms also regulate the mitochondrial respiratory mRNAs in yeast (18). For these studies, we transformed a *cth1*Δ*cth2*Δ yeast strain with plasmids that express either *CTH2*, h*TTP*, or the nonfunctional TZF mutant h*TTP*-C124R, under the control of the iron-regulated *CTH2* promoter. Yeast cells were grown in iron-sufficient or iron-deficient conditions, and the steady-state levels of *NDI1*, *RIP1*, and *ACO1* mRNAs (yeast homologs of *Ndufs1*, *Uqcrfs1*, and *Aco2*, respectively) were determined. As shown in Fig. 4 *F*–*H*, under iron-sufficient conditions, no significant differences were found in the expression of yeast *RIP1*, *NDI1*, or *ACO1* mRNAs in any of the strains. This is consistent with the absence of expression of the TZF proteins in this situation, since the *CTH2* promoter only allows expression under iron-deficient conditions. In contrast, under iron deficiency, *RIP1* and *NDI1* mRNA levels decreased, which was at least partially dependent on the presence of either Cth2 or TTP, whereas expression of nonfunctional TTP-C124R resulted in mRNA levels for these proteins similar to those in the *cth1*Δ*cth2*Δ mutant (vector) (Fig. 4 *F* and *G*). As for *ACO1*, we observed that mRNA levels do not decrease under low iron conditions in cells expressing *CTH2* (Fig. 4*H*), likely due to the role of yeast aconitase in the production of metabolic intermediates for anabolic biosynthesis (19). Importantly, while *ACO1* was induced in the *cth1*Δ*cth2*Δ mutant strain, and in cells expressing *TTP*-C124R, yeasts expressing h*TTP* or *CTH2* were able to suppress *ACO1* mRNA levels under iron-deficient conditions (Fig. 4*H*). These results suggest that TTP can functionally complement CTH2 in the regulation of yeast mitochondrial ETC and TCA-cycle mRNAs and uncover a conserved mechanism for the down-regulation of mitochondrial respiratory function in both yeast and mammals under iron-deficient conditions.

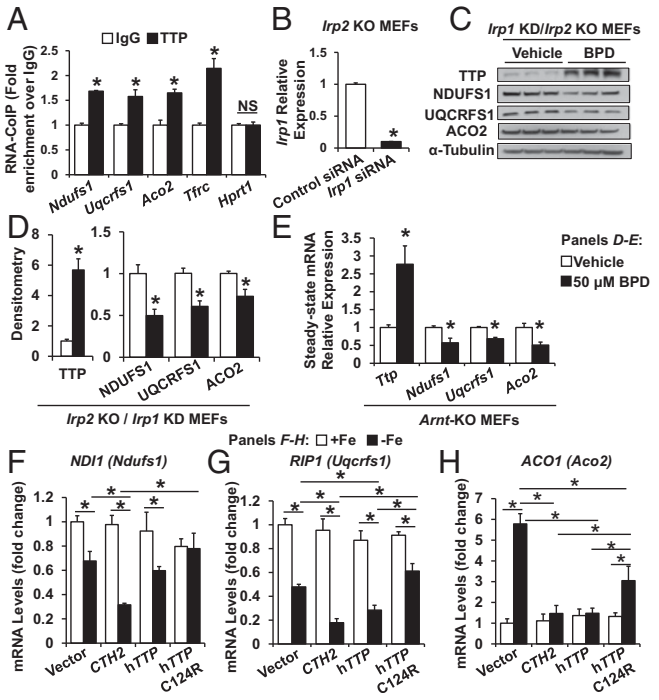

Fig. 4. TTP binds to mRNAs of *Ndufs1*, *Uqcrfs1*, and *Aco2* and regulates their levels independent of the HIF and IRP pathways. (*A*) Levels of *Ndufs1*, *Uqcrfs1*, and *Aco2* mRNA pulled down with indicated antibody. *Tfrc* and Hypoxanthine Phosphoribosyltransferase 1 (*Hprt1*) mRNAs were used as positive and negative controls, respectively. $n = 3$. (*B*) *Irp1* mRNA levels in *Irp2* KO MEFs with KD of *Irp1*. $n = 6$. (*C* and *D*) Western blot (*C*) and densitometry (*D*) of TTP, NDUFS1, UQCRFS1, and ACO2 in *Irp1* KD/*Irp2* KO MEFs in response to BPD. $n = 3$. (*E*) Steady-state mRNA levels of *Ttp*, *Ndufs1*, *Uqcrfs1*, and *Aco2* in *Arnt* KO MEFs with indicated treatment. $n = 3$. (*F*–*H*) mRNA levels of yeast homologs of *Uqcrfs1* (*RIP1*, *F*), *Ndufs1* (*NDI1*, *G*), and *Aco2* (*ACO1*, *H*) in *cth1*Δ*cth2*Δ yeast strain expressing *CTH2* (yeast TTP homolog), WT, or mutant h*TTP*. All graphs show mean ± SEM. $^*P < 0.05$ by ANOVA with Tukey post hoc analysis. NS, not significant.

TTP Is Required for the Regulation of Complex I and III Formation Under Iron Deficiency. UQCRFS1 is an Fe/S-cluster-containing protein and is the last component to be be inserted into the nascent complex III (20). While the insertion of UQCRFS1 is critical for the formation of a stable complex, the subsequent incorporation of the Fe/S cluster into UQCRFS1 is required for forming a functional complex III. Because insertion of the Fe/S cluster only occurs after complex III assembly, it is possible to produce complex III without Fe/S clusters (21, 22). We hypothesized that in iron deficiency TTP acts to suppress *UQCRFS1* expression in parallel with the reduction in cellular iron to prevent the production of apo forms of complex III without the Fe/S cluster. To test this hypothesis, we first assessed the levels of fully assembled complex III in mouse hearts with *Ttp* deletion with and without iron deficiency using blue-native (BN) PAGE. Iron deficiency resulted in a decrease in complex III levels in the hearts of TTP-sufficient *Tnfr1/2*$^{-/-}$ mice, while hearts from *Tnfr1/2*$^{-/-}$/*Ttp*$^{-/-}$ mice displayed no change in complex III levels in iron deficiency (Fig. 5 *A* and *B*), suggesting that TTP is needed for the decrease in the levels of complex III formation in iron deficiency. Additionally, Western blot of BN gels showed that the UQCRFS1 signal (which migrated at the size of complex III) was lower in iron-deficient hearts from *Tnfr1/2*$^{-/-}$ mice when normalized to complex V (which does not contain any TTP-targeted proteins), but not in iron-deficient *Tnfr1/2*$^{-/-}$/*Ttp*$^{-/-}$ hearts (Fig. 5 *C* and *D*). Importantly, we did not observe any free UQCRFS1 (Fig. 5*C*), suggesting that all of the UQCRFS1 is incorporated into complex III in *Tnfr1/2*$^{-/-}$ and *Tnfr1/2*$^{-/-}$/*Ttp*$^{-/-}$ hearts under iron deficiency. Furthermore, the ratio of the UQCRFS1 and UQCRC1 (a non-TTP-targeted, non-Fe/S-cluster-containing member of complex III) signals that migrate with complex III did not change in *Tnfr1/2*$^{-/-}$ and *Tnfr1/2*$^{-/-}$/*Ttp*$^{-/-}$ hearts with and without iron deficiency (Fig. 5 *C* and *E*), indicating that the decrease in UQCRFS1 parallels the change in other protein subunits of complex III in a stoichiometric fashion. Thus, our data indicate that TTP regulates the levels of assembled complex III in iron deficiency by regulating the production of UQCRFS1.

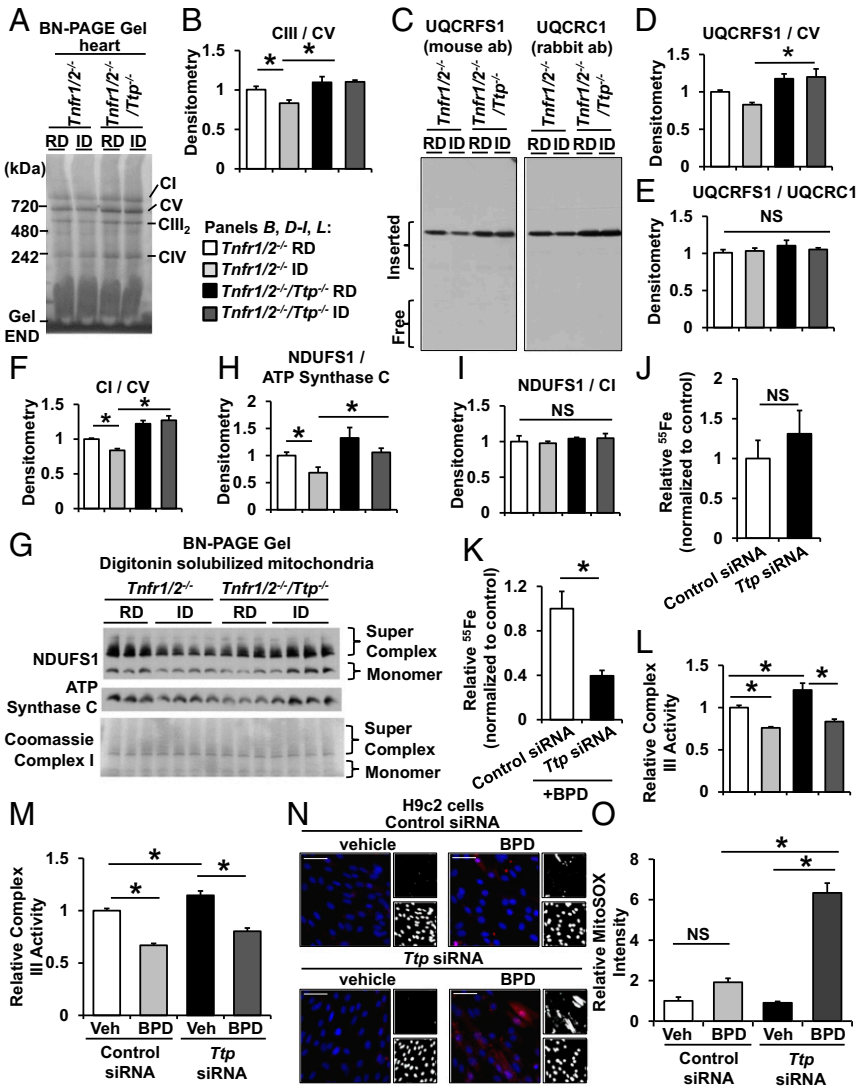

Fig. 5. Deletion of *Ttp* results in the formation of apo-complex III. (*A*) BN gel of mitochondrial lysate from the hearts of *Tnfr1/2*$^{-/-}$ and *Tnfr1/2*$^{-/-}$/*Ttp*$^{-/-}$ mice treated with regular diet (RD) and iron-deficient diet (ID). (*B*) Densitometry of complex III from the native gel in *A* normalized to complex V (CV) in the same gel. (*C*) Native gel immunoblotted for UQCRFS1 and UQCRC1 (another component of complex III that does not bind Fe/S clusters). (*D* and *E*) Densitometry of UQCRFS1 in *C* normalized to CV (*D*) and UQCRFS1 in *C* normalized to UQCRC1 (*E*) in the same blot. (*F*) Densitometry of complex I from the native gel in *A* normalized to complex V in the same gel. (*G*) Native gel of digitonin-extracted mitochondria immunoblotted for NDUFS1 and ATP synthase C (a component of CV) and complex I portion of the same membrane stained with Coomassie G-250. (*H* and *I*) Densitometry of NDUFS1 level normalized to ATP synthase C level (*H*) and NDUFS1 level normalized to complex I level (*I*). (*J* and *K*) Relative ^{55}Fe content in pulled-down UQCRFS1 from HEK293 cells treated with vehicle (*J*) or BPD (*K*) after down-regulation of *Ttp*. A parallel IgG pulldown from the same lysate was used for determining nonspecific binding, and the radioactivity was normalized to UQCRFS1 levels from the same sample as determined by Western blotting. (*L* and *M*) Relative complex III activity in hearts of *Tnfr1/2*$^{-/-}$ and *Tnfr1/2*$^{-/-}$/*Ttp*$^{-/-}$ mice treated with indicated diet (*L*) and in H9c2 cells treated with control or *Ttp* siRNA and with iron chelation for 24 h (*M*). Complex III activity was normalized to citrate synthase activity from the same sample. (*N*) Mitochondrial ROS levels in H9c2 cells treated with control or *Ttp* siRNA and with iron chelation. (*O*) Bar graph summary of *N*. $n = 8$ for *B* and *D*–*F*, 3–4 for *H* and *I*, 4 for *J* and *K*, and 4–6 for *L*–*O*. All graphs show mean ± SEM. *$P < 0.05$ by ANOVA with Tukey post hoc analysis. Veh, vehicle. NS, not significant.

Similar to the relationship between UQCRFS1 and complex III, mitochondrial complex I requires incorporation of NDUFS1 to form a stable complex. Consistent with TTP-mediated suppression of *Ndufs1*, total complex I levels were reduced in mitochondria from *Tnfr1/2*$^{-/-}$ mice under iron deficiency (Fig. 5*F*). Additionally, the intensity of the NDUFS1 band at the molecular weight of complex I and supercomplex (which contains complexes I, III, and IV), when normalized to ATP synthase C at the molecular weight of complex V, was reduced in cardiac mitochondria from *Tnfr1/2*$^{-/-}$ mice under iron deficiency (Fig. 5 *G* and *H*). However, the ratio between the NDUFS1 signal on Western blot and complex I on BN-PAGE remained unchanged (Fig. 5*I*), indicating that total complex I levels matched NDUFS1 levels. However, the levels of both total mitochondrial complex I and NDUFS1 that was incorporated into complex I remained elevated in *Tnfr1/2*$^{-/-}$/*Ttp*$^{-/-}$ hearts under iron deficiency. These findings indicate that TTP also regulates complex I assembly through affecting the production of NDUFS1 protein.

Deletion of TTP Results in the Formation of Apo-Complex III Lacking Fe/S Cluster. Among the three identified targets, UQCRFS1 was the most significantly reduced protein in control cells with iron chelation and remained elevated in the absence of *Ttp* in iron deficiency (Fig. 2*E*). Thus, we focused on UQCRFS1 for the remainder of the studies. To determine whether Fe/S cluster incorporates into UQCRFS1 protein in the absence of TTP, we

then measured incorporation of iron into UQCRFS1 in iron-deficient conditions by preincubating cells with ^{55}Fe nitrilotriacetic acid, followed by TTP down-regulation and iron chelation. For these experiments, we used HEK293 cells to obtain sufficient quantities of mitochondria for immunoprecipitation studies. The amount of radioactivity in immunoprecipitated UQCRFS1, when normalized to UQCRFS1 protein levels from the same sample, was comparable between cells treated with control siRNA or *Ttp* siRNA at baseline (Fig. 5*J*), suggesting that there is sufficient iron to saturate UQCRFS1 protein in both conditions when iron is abundant. However, under iron deficiency, the fraction of iron-containing UQCRFS1 was significantly lower with *Ttp* KD, likely because there is not enough iron available to fully saturate the increased levels of UQCRFS1 in chelated *Ttp* siRNA-treated cells (Fig. 5*K*). We then assessed complex III activity in cardiomyocytes treated with control or *Ttp* siRNA subjected to BPD and in the hearts of *Tnfr1/2*$^{-/-}$ and *Tnfr1/2*$^{-/-}$/*Ttp*$^{-/-}$ mice treated with control or iron deficiency. In this assay, only Fe/S containing complex III will generate activity. Iron deficiency depressed complex III activity in cardiac mitochondria from both *Tnfr1/2*$^{-/-}$ and *Tnfr1/2*$^{-/-}$/*Ttp*$^{-/-}$ hearts and in H9c2 cells treated with control or *Ttp* siRNA (Fig. 5 *L* and *M*). The reduction in complex III activity in control siRNA-treated cells and in *Tnfr1/2*$^{-/-}$ hearts under iron deficiency was expected as we have observed lower levels of total assembled complex III in *Tnfr1/2*$^{-/-}$ mouse hearts under iron deficiency (Fig. 5 *A* and *B*). However, despite an increase in assembled complex III, we observed a reduction of complex III activity under iron deficiency in *Tnfr1/2*$^{-/-}$/*Ttp*$^{-/-}$ hearts and in *Ttp* siRNA-treated cells, indicating that some of the assembled complex IIIs are dysfunctional. These results suggest that in the absence of TTP and under iron deficiency a portion of the assembled complex III does not contain Fe/S clusters, while in conditions of intact TTP levels the majority of remaining complex III retains its iron and contributes to activity.

Deletion of TTP Results in a Reduction in Mitochondrial Respiration. Since reduced ETC activity can lead to reduced oxygen usage, we next measured oxygen consumption rate (OCR). For these studies, we treated H9c2 cells with control and *Ttp* siRNA in the presence and absence of iron deprivation. Under iron deficiency, both control and *Ttp* siRNA-treated cells demonstrated lower oxygen consumption, which was accentuated at the addition of carbonyl cyanide 3-chlorophenylhydrazone (which measures maximal oxygen consumption) (*SI Appendix*, Fig. S6 *A* and *B*). Deletion of *Ttp* resulted in a further reduction in baseline and maximal OCR in iron deficiency (*SI Appendix*, Fig. S6 *A* and *B*). The change in oxygen consumption was not due to altered mitochondrial content, as mitochondrial DNA levels were comparable among cells treated with control or *Ttp* siRNA with and without iron deficiency (*SI Appendix*, Fig. S6*C*).

To determine if similar changes occur in vivo, we studied OCR in freshly isolated mitochondria from *Tnfr1/2*$^{-/-}$ and *Tnfr1/2*$^{-/-}$/*Ttp*$^{-/-}$ hearts with and without iron deficiency. Mitochondrial state III respiration driven by pyruvate/malate (complex I and III) was significantly higher in *Tnfr1/2*$^{-/-}$/*Ttp*$^{-/-}$ hearts compared with *Tnfr1/2*$^{-/-}$ hearts when mice are fed normal chow (*SI Appendix*, Fig. S6*D*). Under iron-replete conditions, *Tnfr1/2*$^{-/-}$/*Ttp*$^{-/-}$ hearts also exhibit a trend toward increased maximum respiratory capacity when mitochondria were fueled with pyruvate and malate (*SI Appendix*, Fig. S6*E*). This is consistent with increased complex III activity as well as increased complex I assembly in the absence of TTP (Fig. 5 *B*, *F*, *K*, and *L*). We also observed similar baseline changes when mitochondria were fueled with succinate (complex II and III) and complex I respiration inhibited by rotenone (*SI Appendix*, Fig. S6 *F* and *G*). Iron deficiency resulted in reduction of state III and maximal oxygen consumption in both *Tnfr1/2*$^{-/-}$ and *Tnfr1/2*$^{-/-}$/*Ttp*$^{-/-}$ hearts, but the relative reduction was greater in *Tnfr1/2*$^{-/-}$/*Ttp*$^{-/-}$ hearts (*SI Appendix*, Fig. S6 *D*–*G*). This is consistent with our observation in cultured cells and further supports that some of the mitochondrial assembled complexes are dysfunctional in *Tnfr1/2*$^{-/-}$/*Ttp*$^{-/-}$ hearts. Taken together, our in vitro and in vivo data indicate that deletion of TTP leads to more severe mitochondrial dysfunction in iron deficiency.

Since Cth2 and TTP regulate similar mitochondrial targets (Fig. 4 *F*–*H*), we then assessed whether induction of *CTH2* under iron deficiency also regulates mitochondrial ETC complexes and cellular respiration. Using cellular oxygen consumption as a surrogate marker for ETC activity, we observed a reduction in oxygen consumption in *cth1*Δ*cth2*Δ yeast expressing *CTH2* under its endogenous promoter and grown under iron deficiency (*SI Appendix*, Fig. S6*H*). These findings are expected since mitochondrial ETC is dependent on iron, and several of its key components are regulated by Cth2. However, in *cth1*Δ*cth2*Δ yeast cells (vector), we also observed a similar decrease in oxygen consumption (*SI Appendix*, Fig. S6*H*). This finding indicates that under prolonged and severe iron deficiency other regulatory mechanisms, in addition to Cth2, can inhibit respiration. This is consistent with a previous report, which demonstrates that the drop in heme levels that occurs in iron-deficient conditions leads to a decrease in the transcription of the mitochondrial electron carrier cytochrome *c* (*CYC1* in yeast) (23), and our observation of reduced expression of *NDI1* and *RIP1* in cells lacking both *CTH1* and *CTH2* (Fig. 4 *F* and *G*). Therefore, to bypass other mechanisms that repress respiration in iron deficiency, we overexpressed *CTH2* in iron-sufficient conditions by using a yeast constitutive promoter (CTH2^{OE} cells). As shown in *SI Appendix*, Fig. S6*I*, *CTH2* expression in iron sufficiency diminishes oxygen consumption, which does not occur when a cysteine residue within Cth2 TZF is mutagenized (CTH2-C190R^{OE} cells). Collectively, our results indicate that yeast family members of TTP promote the repression of mitochondrial respiration under iron deficiency.

Production of Apo-UQCRFS1 Under Iron Deficiency and in the Absence of TTP Results in Increased ROS Production. Apo-UQCRFS1 without the required Fe/S cofactor would lack critical electron transport capability and, as a result, its insertion into the ETC could cause electron leakage and oxidative stress. Thus, we next asked whether the production of apo-UQCRFS1 without Fe/S clusters would result in ROS production under iron-deficiency conditions. Indeed, significantly more mitochondrial oxidant production was observed in H9c2 cells with *Ttp* KD and iron deficiency than in WT cells, while iron deficiency in control siRNA-treated H9c2 did not change mitochondrial ROS levels (Fig. 5 *N* and *O*). These results demonstrate that TTP is required to mitigate the increased ROS under iron deprivation.

A previous study demonstrated that complete loss of UQCRFS1 by gene KO resulted in increased mitochondrial ROS production (24). In our system of reduced UQCRFS1 protein levels (through regulation by TTP under iron deficiency) we did not observe an increase mitochondrial ROS (Fig. 5 *N* and *O*). We hypothesized that this discrepancy could be due to differences in the degree of reduction in UQCRFS1. Therefore, to determine if a decrease (but not complete ablation) of UQCRFS1 levels would influence mitochondrial ROS production in the iron-replete state, we overexpressed either WT (h*TTP*) or TZF-inactive *TTP* mutant (C124R) in H9c2 cells. Overexpression of TTP resulted in about 30% reduction in UQCRFS1 protein levels (*SI Appendix*, Fig. S3 *E* and *F*), comparable to the effect of BPD on UQCRFS1 protein levels (Figs. 2 *B* and *E* and 4 *C* and *D*). Similar to iron chelation, TTP overexpression did not significantly alter mitochondrial ROS (*SI Appendix*, Fig. S7), suggesting that mild reductions in UQCRFS1 protein levels alone are not sufficient to induce mitochondrial ROS production.

Although incorporation of apo-complex III into the ETC can result in an overall increase in mitochondrial ROS, the specific source of the ROS can vary. Thus, we studied the site of increased mitochondrial ROS production. We used malate plus glutamate as substrates in the presence of the complex III inhibitor myxothiazol to assess ROS production through complex I, and succinate plus rotenone and myxothiazol to assess ROS

production through complex II (rotenone was used to block reverse electron transport through complex I and myxothiazol to block electron delivery to complex III). We showed that ROS production from both complexes I and II were increased in iron-deficient cells in the absence of TTP compared with iron-deficient cells treated with control siRNA (Fig. 6 *A* and *B*). To determine ROS production from complex III alone, we first incubated mitochondria with succinate, rotenone, and antimycin A (which measures ROS production from complex II and III) and then added the complex III inhibitor myxothiazol. The difference in the ROS production rate before and after the addition of myxothiazol reflects the ROS production rate from complex III alone. We observed no difference in complex III ROS production under iron deficiency in the absence of TTP, which is consistent with the inability of electrons to be delivered to apo-complex III (complex III without Fe/S clusters) (Fig. 6*C*). Thus, in the absence of TTP, iron deprivation leads to increased ROS production from complexes I and II. This increase in mitochondrial ROS was not associated with a change in the mitochondrial membrane potential (*SI Appendix*, Fig. S8 *A* and *B*).

Since ROS can damage Fe/S clusters in mitochondrial aconitase and halt the TCA cycle, we next measured mitochondrial aconitase activity in H9c2 cardiomyoblasts treated with *Ttp* siRNA with and without iron deficiency. *Ttp* siRNA-treated cells exhibited increased mitochondrial aconitase activity at baseline, consistent with TTP regulating the mitochondrial aconitase mRNA. Iron deficiency in control siRNA-treated cells resulted in lower mitochondrial aconitase activity but led to a further decrease in *Ttp* KD cells despite higher protein levels (Fig. 6*D*). Similar findings were observed in heart tissue from *Tnfr1/2*$^{-/-}$ and *Tnfr1/2*$^{-/-}$/*Ttp*$^{-/-}$ mice with and without iron deficiency (Fig. 6*E*). Since aconitase activity was normalized to citrate synthase activity in the same sample, our results are not due to changes in mitochondrial mass. Also, control and *Ttp* KD cells have similar extent of iron deficiency, so the further reduction of mitochondrial aconitase activity in *Ttp* KD cells would be consistent with increased damage to Fe/S clusters in mitochondrial aconitase by ROS. We also observed that *Ttp* deletion is associated with increased cell death in iron deficiency in neonatal rat cardiomyocytes (Fig. 6*F*), indicating that the oxidative stress associated with *Ttp* deletion is detrimental to the cell.

Apo-UQCRFS1 and Oxidative Stress Mediate Cell Death and Reduced OCR in Iron Deficiency. To determine the causal role of apo-UQCRFS1 in the observed oxidative stress, we titrated *Uqcrfs1* siRNA in cells treated with control or *Ttp* siRNA and BPD, such that *Uqcrfs1* and *Ttp* double-KD cells would have UQCRFS1 levels comparable to those of control siRNA-treated cells (Fig. 6*G*). Mitochondrial ROS levels with iron deficiency were almost completely reversed in *Uqcrfs1* and *Ttp* double-KD cells compared with *Ttp* KD cells (Fig. 6 *H* and *I*). This finding suggests that increased production of UQCRFS1 in *Ttp* KD cells under iron deficiency leads to increased ROS production.

We then studied the contribution of ROS production to the impairment of mitochondrial respiration and cell viability in cells with *Ttp* deletion and iron chelation. *Ttp* KD cells with iron deficiency were treated with the mitochondrial-targeted antioxidant mitoTempo, followed by measurement of oxygen consumption and cell death. MitoTempo treatment resulted in a significant increase in baseline oxygen consumption and a partial reversal in maximal oxygen consumption in *Ttp* KD cells under iron deficiency (*SI Appendix*, Fig. S8 *C* and *D*). The partial reversal of oxygen consumption with mitoTempo treatment is consistent with our hypothesis that increased ROS, which can damage other ETC components and depress oxygen consumption, is partially responsible for the depressed respiration in *Ttp* KD cells under iron deficiency. However, the lack of complete reversal suggests that in addition to oxidative damage, electron leak due to lack of adequate Fe/S clusters in complex III also contributes to reduced oxygen consumption with *Ttp* KD and iron chelation. Additionally, increased cell death with *Ttp* KD

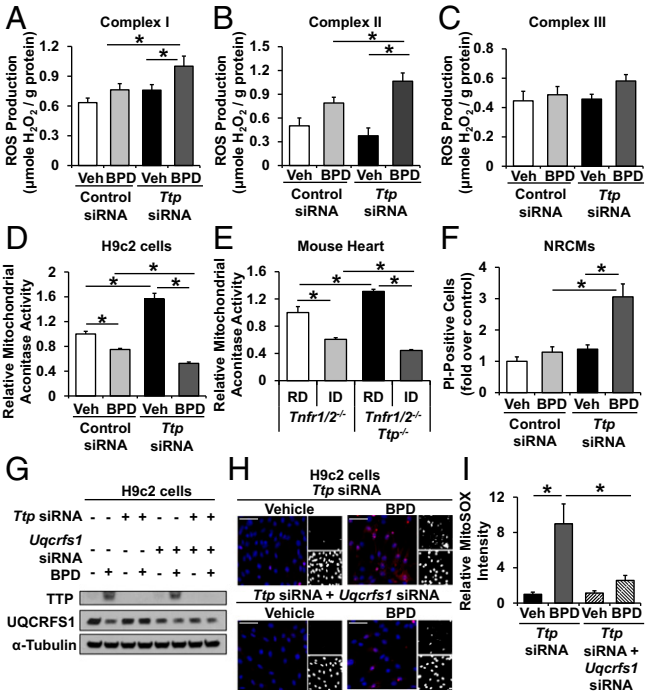

Fig. 6. Mitochondrial complex I and II contribute to ROS production with *Ttp* deletion and iron deficiency. (*A–C*) ROS production by mitochondrial complex I (*A*), complex II (*B*), and complex III (*C*) in isolated mitochondria from H9c2 cells with indicated treatment. (*D* and *E*) Relative mitochondrial aconitase activity in H9c2 cells with indicated treatment (*D*) and in hearts of *Tnfr1/2*$^{-/-}$ and *Tnfr1/2*$^{-/-}$/*Ttp*$^{-/-}$ mice treated with indicated diet (*E*). (*F*) Iron deficiency and TTP deletion is associated with increased cell death in neonatal rat cardiomyocytes (NRCMs). (*G*) H9c2 cells with double KD of *Uqcrfs1* and *Ttp*; siRNA was titrated such that *Uqcrfs1* and *Ttp* double-KD cells and control siRNA-treated cells have comparable UQCRFS1 levels under iron deficiency. (*H* and *I*) Representative images (*H*) and summary bar graph (*I*) of MitoSOX Red fluorescence signals in H9c2 cells treated with indicated siRNA. (Scale bars, 100 μm.) Upper right shows positive red fluorescence signal in black and white scale and lower right shows nuclear staining by Hoechst in black-and-white scale. $n = 3$ for *A–C*, *G*, and *H*, 7 for *D*, and 4–6 for *E*. All graphs show mean ± SEM. $^*P < 0.05$ by ANOVA with Tukey post hoc analysis. Veh, vehicle.

under iron deficiency was reversed with mitoTempo treatment (*SI Appendix*, Fig. S8*E*), suggesting that increased ROS production contributes to cell death in the setting of iron chelation and *Ttp* KD.

Deletion of TTP Results in Alteration of Cellular Metabolism. Since mitochondrial oxidative phosphorylation is a major source of cellular ATP production, we next studied whether TTP-mediated changes in mitochondrial oxidative phosphorylation cause a shift in cellular energetics. *Ttp* KD cells under iron deficiency have intracellular ATP levels comparable to control-siRNA treated cells under iron deficiency (*SI Appendix*, Fig. S9*A*), suggesting that they are not under energetic stress. This is likely due to a compensatory up-regulation of glycolysis, as evidenced by higher lactate production in *Ttp* KD cells under iron deficiency (*SI Appendix*, Fig. S9*B*).

We also measured ATP levels in *Tnfr1/2*$^{-/-}$ and *Tnfr1/2*$^{-/-}$/*Ttp*$^{-/-}$ mice. Both *Tnfr1/2*$^{-/-}$ and *Tnfr1/2*$^{-/-}$/*Ttp*$^{-/-}$ mice exhibited no cardiac energetic stress, as cardiac ATP content was comparable in these mice with and without iron deficiency (*SI Appendix*, Fig. S9*C*). To determine if up-regulation of glycolysis also occurs in vivo under iron deficiency, we performed metabolomic studies on cardiac tissue from these mice. Iron deficiency resulted in accumulation of dihydroxyacetone phosphate, phosphoenolpyruvate, and lactate in both *Tnfr1/2*$^{-/-}$ and *Tnfr1/2*$^{-/-}$/*Ttp*$^{-/-}$ hearts, consistent with increased glycolytic flux (*SI Appendix*,

Fig. S9*D*). Similar to the in vitro data, *Tnfr1/2*$^{-/-}$/*Ttp*$^{-/-}$ hearts accumulated more lactate under iron deficiency. The increased glycolysis was not due to reduced mitochondrial mass, as *Tnfr1/2*$^{-/-}$ and *Tnfr1/2*$^{-/-}$/*Ttp*$^{-/-}$ mice with and without iron deficiency displayed a comparable number of mitochondria (as assessed by electron microscopy) and similar mitochondrial DNA content (*SI Appendix*, Fig. S9 *E* and *F*). Thus, under iron deficiency, glycolysis is up-regulated to compensate for the lower mitochondrial ETC activity and energy production.

Deletion of TTP Leads to Cardiac Damage in Iron Deficiency. While high-output heart failure may occur in iron deficiency secondary to severe anemia, iron deficiency does not directly lead to CM. Given the role of TTP in mitochondrial function, ROS production, and cell viability in iron deficiency, we then asked whether deletion of *Ttp* (and the resultant unchecked generation of UQCRFS1 without the required Fe/S clusters) would result in oxidative stress, cellular dysfunction, and CM in mice with iron deficiency. *Tnfr1/2*$^{-/-}$/*Ttp*$^{-/-}$ mice displayed a significant decline in the left ventricular (LV) ejection fraction (EF), LV fractional shortening (FS), and a small but significant increase in diastolic LV wall thickness (sum of anterior and posterior wall thickness) 6 wk after initiation of iron-deficient diet, but this was not observed in *Tnfr1/2*$^{-/-}$ mice (Fig. 7 *A*–*D*). To determine if the phenomenon is related to the gene dosage of TTP, we also subjected mice with heterozygous deletion of *Ttp* (*Tnfr1/2*$^{-/-}$/*Ttp*$^{+/-}$ mice) to the same iron-deficiency protocol. Despite a similar extent of iron deficiency (*SI Appendix*, Fig. S4 D–K), *Tnfr1/2*$^{-/-}$/*Ttp*$^{+/-}$ mice did not develop systolic dysfunction (Fig. 7 *B*–*D*). *Tnfr1/2*$^{-/-}$/*Ttp*$^{-/-}$ mice also displayed a trend toward increased heart weight (HW)/BW and a significant increase in HW/TL under iron-deficiency conditions (Fig. 7 *E* and *F*). These findings collectively suggest that the loss of TTP is detrimental to cardiac function under iron deficiency. No correlation between Hgb and LVEF was noted in either *Tnfr1/2*$^{-/-}$ or *Tnfr1/2*$^{-/-}$/*Ttp*$^{-/-}$ mice (Fig. 7*G*), confirming that the slightly greater reductions in Hgb and HCT in the *Tnfr1/2*$^{-/-}$/*Ttp*$^{-/-}$ mice are not responsible for the reduction in EF. Histological analysis of the cardiac tissue of these mice revealed no infiltration of inflammatory cells or fibrosis (Fig. 7*H*), confirming that inflammation is not a main contributor to development of CM in the *Tnfr1/2*$^{-/-}$/*Ttp*$^{-/-}$ mice with iron deprivation. Additionally, the contractile dysfunction seen in iron-deficient *Tnfr1/2*$^{-/-}$/*Ttp*$^{-/-}$ mice was not due to insufficient energy production, as hearts from iron-deficient *Tnfr1/2*$^{-/-}$ and *Tnfr1/2*$^{-/-}$/*Ttp*$^{-/-}$ mice have comparable ATP levels (*SI Appendix*, Fig. S9*C*). Finally, hearts from *Tnfr1/2*$^{-/-}$/*Ttp*$^{-/-}$ mice with iron deprivation displayed higher levels of lipid peroxidation (Fig. 7*I*), consistent with higher oxidative stress. To demonstrate that the CM under iron deficiency is due to specific loss of *Ttp* in cardiomyocytes, we also generated mice with cardiomyocyte-specific deletion of *Ttp* (cs-*Ttp*$^{-/-}$, cs-*Ttp* KO) by breeding *Ttp*$^{f/f}$ mice with *Myh6*-Cre transgenic mice. After the same iron-deficiency protocol, control (Cre^{-} TTP$^{f/f}$, cs-*Ttp* WT) and cs-*Ttp* KO mice demonstrated a comparable level of iron deficiency, as assessed by Hgb and serum and tissue iron measurement (*SI Appendix*, Fig. S10 *A*–*H* and Table S3). Similar to the *Tnfr1/2*$^{-/-}$/*Ttp*$^{-/-}$ mice, cs-*Ttp* KO mice exhibited systolic dysfunction (*SI Appendix*, Fig. S10 *I*–*M*). These results suggest that TTP is essential for the normal cardiac response to iron deficiency, and that its deletion leads to increased oxidative stress and CM.

Discussion

Cellular iron deficiency has been shown to activate the IRP pathway, leading to increased cellular uptake of iron. However, when the IRP pathway does not provide sufficient iron to keep up with cellular demand, cells face conditions in which iron becomes scarce and iron conservation becomes a priority. How cells respond to persistent intracellular iron deficiency that is not resolved despite IRP activation remains unclear. It is now apparent that the IRP pathway is not the sole mediator of the cellular response to iron deficiency, and that other pathways are essential for ensuring cell survival in extreme iron deficiency. Previous work has shown that deletion of TTP leads to cell death in response to iron deficiency (8); however, the exact mechanism by which TTP ensures cellular survival in iron deficiency has not been elucidated. We hypothesized that TTP optimizes iron utilization by the cell when iron levels are low by preferentially suppressing production of iron-containing proteins participating in nonessential cellular pathways. To test this hypothesis, we focused on mitochondrial oxidative phosphorylation as a pathway that consumes significant amounts of cellular iron in the form of Fe/S clusters and heme but is not essential for cellular survival, at least in the short term, due to glycolysis' being a readily available substitute that does not require iron. Our results show that TTP targets UQCRFS1, a Fe/S-cluster-containing component of complex III. Up-regulation of TTP in iron deficiency results in reduced production of UQCRFS1, which appears to precisely match the amount of iron available in the cells and may serve at least two purposes: (*i*) to reduce iron consumption by the mitochondrial ETC to make iron available for other cellular processes and (*ii*) to minimize the amount of apo-UQCRFS1 (without its Fe/S cluster cofactor) that can be incorporated into complex III, which would optimize electron movement through the ETC and decrease ROS production by the complex. Overall, we present evidence that TTP not only appears to conserve iron by shunting it away from at least one nonessential pathway (mitochondrial oxidative phosphorylation) but also fine-tunes the operation of this pathway in iron-deficient conditions.

According to the ExAC database (exac.broadinstitute.org/), most of the documented missense mutations in *TTP* are heterozygote mutations, and to our knowledge there have not been any homozygote loss-of-function mutations documented in the *TTP* gene in humans. If individuals carrying homozygous mutations of *TTP* actually exist, it is conceivable that these individuals will have severe systemic inflammation (due to TTP regulation of TNFα), and they will not develop CM unless they are also severely iron-deficient. However, carriers of *TTP* heterozygote mutations are not likely to develop CM even under severe iron deficiency, as evidenced by the preserved cardiac function of the heterozygote *Ttp* KO mice under iron deficiency. It would be of great interest to perform association studies between iron deficiency and CM to determine if specific polymorphisms are associated with predisposition to CM due to hypomorphic *TTP*.

Our results indicate that TTP targets one component of complex I (*NDUFS1*) and one component of complex III (*UQCRFS1*). Complex I contains 14 core proteins, including NDUFS1, and an additional 34 subunit proteins (25), while complex III contains 11 proteins with UQCRFS1 as one of the three respiratory subunits (26). It is interesting that TTP only targets one of the proteins in each of these complexes. This may be due to several reasons. First, NDUFS1 and UQCRFS1 are both Fe/S-cluster-containing proteins, and TTP reduces their levels in parallel with the reduction in cellular Fe/S levels. Second, NDUFS1 and UQCRFS1 are integral components of complexes I and III, respectively. Incorporation of UQCRFS1 into complex III is one of the final steps in both yeast and mammalian cells and is required for complex stability (20, 24, 27). Thus, if UQCRFS1 levels are reduced, the nascent complex III is destabilized and an apo-complex III will not be formed (24). Additionally, a reduction in NDUFS1 protein levels also prevents formation of complex I and its association into supercomplexes (28, 29). Therefore, the TTP regulatory mechanism can significantly impact the formation of individual respiratory chain complexes and their association into a supercomplex.

A critical property of mitochondrial ETC complexes is their capacity to assemble into supercomplexes. Supercomplex formation has been shown to increase the efficiency of electron delivery between different complexes and prevent ROS formation (30, 31). Respiratory chain supercomplex assembly begins with the interaction among complex III, complex IV, and the membrane arm of complex I and is subsequently followed by the association of the matrix arm of complex I (also known as the "n

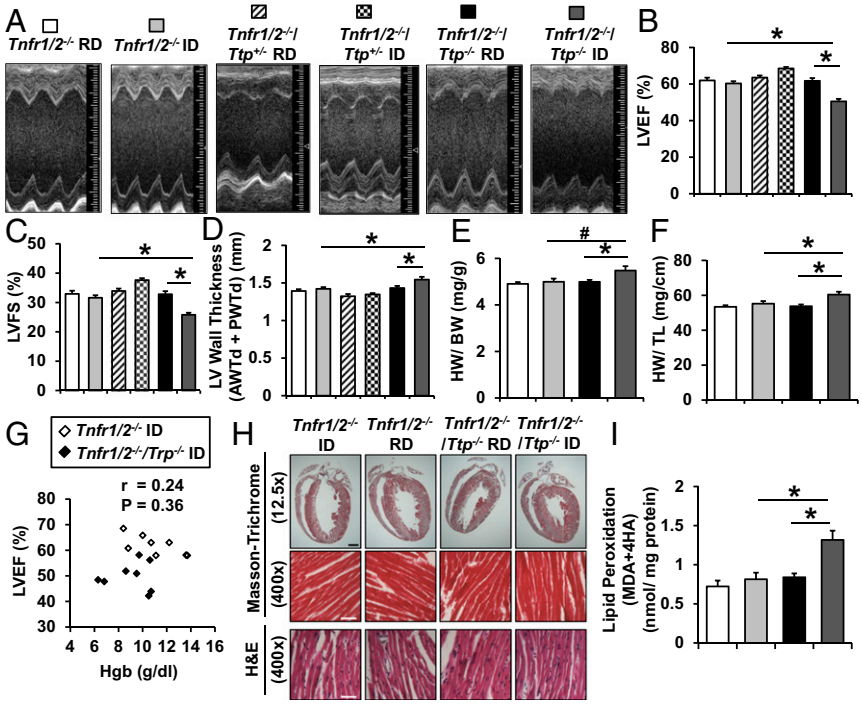

Fig. 7. *Tnfr1/2*$^{-/-}$*/Ttp*$^{-/-}$ mice display decreased cardiac function in iron deficiency. (*A*) Two-dimensional cardiac images of *Tnfr1/2*$^{-/-}$, *Tnfr1/2*$^{-/-}$*/Ttp*$^{+/-}$, and *Tnfr1/2*$^{-/-}$*/Ttp*$^{-/-}$ mice treated with regular diet (RD) and iron-deficient diet (ID). (*B–D*) LVEF (*B*), LVFS (*C*), and LV wall thickness (*D*) as assessed by echocardiography in *Tnfr1/2*$^{-/-}$, *Tnfr1/2*$^{-/-}$*/Ttp*$^{+/-}$, and *Tnfr1/2*$^{-/-}$*/Ttp*$^{-/-}$ mice treated with indicated diet. (*E* and *F*) HW-to-BW ratio (*E*) and HW-to-TL ratio (*F*) in *Tnfr1/2*$^{-/-}$ and *Tnfr1/2*$^{-/-}$*/Ttp*$^{-/-}$ mice in the presence and absence of iron deficiency. (*G*) Correlation between Hgb and LVEF in *Tnfr1/2*$^{-/-}$ and *Tnfr1/2*$^{-/-}$*/Ttp*$^{-/-}$ mice treated with ID. (*H*) Masson's trichrome and H&E staining of hearts from *Tnfr1/2*$^{-/-}$ and *Tnfr1/2*$^{-/-}$*/Ttp*$^{-/-}$ mice after RD or ID, demonstrating lack of fibrosis. (Scale bars: black scale, 1 mm and white scale, 50 μm.) (*I*) Oxidative stress, as assessed by lipid peroxidation, in the hearts of *Tnfr1/2*$^{-/-}$ and *Tnfr1/2*$^{-/-}$*/Ttp*$^{-/-}$ mice treated with RD or ID. n = 6–12 for *B–F* and 3 for *I*. All graphs show mean ± SEM. $^{*}P < 0.05$ and $^{\#}P < 0.1$ by ANOVA with Tukey post hoc analysis.

module," which contains the catalytic unit of complex I) (32). Ultimately, supercomplex formation requires fully assembled complex III and specifically Fe/S-cluster-bound NDUFS1 in complex I. Notably, the addition of Fe/S clusters to complex III is not required. Therefore, a shift toward the apo form of UQCRFS1, as caused by cellular iron deficiency in the absence of TTP, can lead to formation of supercomplexes in which remaining holo-NDUFS1 and apo-UQCRFS1 are both present. We hypothesize that this could lead to ROS production in two ways. First, electrons would enter fully formed holo-complex I but ultimately get trapped and leaked as they would have no way of progressing through apo-complex III. Second, electrons delivered to complex II can generate ROS through reverse electron transport to either fully assembled complex I or complex I containing only the membrane portion. It should be noted that even under severe iron deficiency complex II can still receive electrons for a few reasons. First, the Krebs cycle is slowed but not fully halted, as evidenced by the decreased but not terminated oxygen consumption under iron deficiency. This is likely due to the presence of some (albeit fewer) functional ETC components with a slower turnover of the NADH and $FADH_2$. Additionally, while being less efficient, electrons generated from glycolysis can still be delivered directly to complex II via the glycerophosphate shuttle (33). This pathway may even have a higher contribution to transfer electrons from glycolysis into the ETC under iron deficiency because slower TCA cycle turnover renders the malate–aspartate shuttle less efficient. ROS production from the aforementioned two mechanisms can damage remaining normal supercomplexes and cause their dissociation (34). We propose that TTP plays a crucial role in downregulating proteins like UQCRFS1 and NDUFS1 to minimize the production of apo-supercomplexes and free complex I which have higher capacities for ROS production (35). Otherwise, increased ROS production can in turn damage or dissociate other complexes and further amplify ROS production, culminating in cell death.

While our data support NDUFS1's being a target of TTP, NDUFS1 protein levels are also reduced in *Ttp* KD cells under iron deficiency. This suggest that there is both TTP-dependent and -independent regulation of NDUFS1 under iron deficiency. We also observed a similar phenomenon in yeast, where iron deficiency regulates *NDI1* expression even in the absence of Cth1 and Cth2 (yeast homologs of TTP) (Fig. 4*F*). This iron-dependent but TTP-independent mechanism is likely to be more relevant in severe iron deficiency, such as our in vitro model. In contrast, in vivo diet-induced iron deficiency is likely to be more moderate (as evidenced by lower reduction of cellular iron in our in vivo model vs. in vitro data), so we did not observe this iron-dependent but TTP-independent regulation on NDUFS1 in the mouse tissue. The additional regulatory mechanism of complex I in iron deficiency in the mammalian system is not currently known.

Our studies identify mitochondrial oxidative phosphorylation as an iron-consuming process that can be restricted under iron deficiency. It should be noted that while mitochondrial oxidative phosphorylation is reduced under iron deficiency, the mitochondria is not completely shut down. While a complete inhibition of mitochondrial respiration (for example through pharmacological inhibitors or genetic deletion of ETC components) would lead to cellular energy crisis and impair cardiac contractile function, our data indicate that the mild inhibition of mitochondrial respiration under iron deficiency is compensated by concurrent up-regulation of glycolysis to maintain the cellular ATP pool. This would explain why WT animals under iron deficiency did not have overt cardiac dysfunction due to lack of energy source. TTP-mediated decrease in iron-consuming proteins in the ETC under iron deficiency would free up the cellular iron pool for other iron-consuming pathways. It is conceivable that certain iron-containing pathways essential for cell survival would not be down-regulated during iron deficiency and would have access to this iron pool. Although it would be of great interests to identify these "essential" pathways, to date there is no unbiased approach to systematically examine the presence of iron in all iron-consuming pathways. Of note, it has also been proposed that yeast cells do not possess a specific mechanism that preferentially allocates iron to certain cellular pathways, and that iron incorporation into proteins is primarily determined by the amount of apo-protein available in the cells (36). Additionally, other regulatory mechanisms increase the function of essential iron-containing proteins in iron-deficient yeast cells (37). It remains to be determined if TTP promotes an essential pathway through a similar mechanism.

Our findings suggest that the role of TTP in iron regulation may extend beyond a single cell and to the level of a whole organism, and that this protein may function in iron redistribution

between different tissues or organs. Specific iron-requiring pathways may be more or less "essential" for cellular survival in iron deficiency, and, similarly, the impact of iron deficiency in various tissues on the survival of a whole organism may also be profoundly different. For example, insufficient iron levels inside a skeletal muscle will lead to reductions in myoglobin and suppression in oxidative phosphorylation. While this results in decreased force of contraction, this may be significantly less detrimental to the whole organism than lower levels of iron within cardiac muscle given subsequent impairment in contractility and inability to maintain proper circulation. Thus, by preferentially regulating cellular iron transporters, such as *TFRC*, TTP may specifically prevent iron uptake in certain, less "essential" tissues, to increase its availability in the blood to be taken up by more "vital" organs through the activity of the IRP1/2 system. Further studies are needed to confirm or refute this hypothesis.

In summary, our results demonstrate a pathway that is activated in response to iron deficiency. This pathway leads to a reduction in the production of critical proteins in complexes I and III and balances the levels of these proteins with those of Fe/S cluster levels. Disruption of this pathway in the heart leads to oxidative stress, cellular damage, and, ultimately, CM.

Methods

All animal studies were approved by the Institutional Animal Care and Use Committee at Northwestern University and were performed in accordance with guidelines from the National Institutes of Health. Molecular studies were performed according to routine protocol previously published by our group. Unpaired two-tailed Student's *t* tests or one-way ANOVA were used to determine statistical significance. $P < 0.05$ was considered to be statistically significant, as indicated by an asterisk. Significant one-way ANOVA is followed by Tukey post hoc analysis. For detailed in vivo and in vitro experimental methods, see *SI Appendix, SI Methods*.

ACKNOWLEDGMENTS. We thank Kai Xu, Meng Shang, and Eric Xia for genotyping and animal husbandry; Arineh Khechaduri for technical help; and Lisa Wilsbacher and Paul Burridge for critical suggestions on the paper. This work was supported by NIH Grants R01 HL127646, HL140973, and HL138982 (to H.A.), a predoctoral contract from the Spanish Ministry of Economy, Industry and Competitiveness (Mineco) (L.R.-A.), Mineco Grants BIO2014-56298-P and BIO2017-87828-C2-1-P and the European Regional Development Fund (S.P.), and Grant AICO/2015/004 from the Generalitat Valenciana (to M.T.M.-P.). Metabolomics studies were performed by the Metabolomics Core Facility at the Robert H. Lurie Comprehensive Cancer Center of Northwestern University. Electron microscopy was performed at the Northwestern University Center for Advanced Microscopy generously supported by National Cancer Institute Cancer Center Support Grant P30 CA060553 awarded to the Robert H. Lurie Comprehensive Cancer Center.

1. McLean E, Cogswell M, Egli I, Wojdyla D, de Benoist B (2009) Worldwide prevalence of anaemia, WHO Vitamin and Mineral Nutrition Information System, 1993-2005. *Public Health Nutr* 12:444–454.
2. Pantopoulos K (2004) Iron metabolism and the IRE/IRP regulatory system: An update. *Ann N Y Acad Sci* 1012:1–13.
3. Rouault TA (2006) The role of iron regulatory proteins in mammalian iron homeostasis and disease. *Nat Chem Biol* 2:406–414.
4. Abboud S, Haile DJ (2000) A novel mammalian iron-regulated protein involved in intracellular iron metabolism. *J Biol Chem* 275:19906–19912.
5. Eisenstein RS (2000) Iron regulatory proteins and the molecular control of mammalian iron metabolism. *Annu Rev Nutr* 20:627–662.
6. Ponka P, Beaumont C, Richardson DR (1998) Function and regulation of transferrin and ferritin. *Semin Hematol* 35:35–54.
7. Thomson AM, Rogers JT, Leedman PJ (1999) Iron-regulatory proteins, iron-responsive elements and ferritin mRNA translation. *Int J Biochem Cell Biol* 31:1139–1152.
8. Bayeva M, et al. (2012) mTOR regulates cellular iron homeostasis through tristetraprolin. *Cell Metab* 16:645–657.
9. Brooks SA, Blackshear PJ (2013) Tristetraprolin (TTP): Interactions with mRNA and proteins, and current thoughts on mechanisms of action. *Biochim Biophys Acta* 1829: 666–679.
10. Bayeva M, Chang HC, Wu R, Ardehali H (2013) When less is more: Novel mechanisms of iron conservation. *Trends Endocrinol Metab* 24:569–577.
11. Stehling O, Sheftel AD, Lill R (2009) Chapter 12 Controlled expression of iron-sulfur cluster assembly components for respiratory chain complexes in mammalian cells. *Methods Enzymol* 456:209–231.
12. Robergs RA, Ghiasvand F, Parker D (2004) Biochemistry of exercise-induced metabolic acidosis. *Am J Physiol Regul Integr Comp Physiol* 287:R502–R516.
13. Carballo E, Blackshear PJ (2001) Roles of tumor necrosis factor-alpha receptor subtypes in the pathogenesis of the tristetraprolin-deficiency syndrome. *Blood* 98: 2389–2395.
14. Cho EA, et al. (2013) Differential in vitro and cellular effects of iron chelators for hypoxia inducible factor hydroxylases. *J Cell Biochem* 114:864–873.
15. Peyssonnaux C, et al. (2007) Regulation of iron homeostasis by the hypoxia-inducible transcription factors (HIFs). *J Clin Invest* 117:1926–1932.
16. Puig S, Askeland E, Thiele DJ (2005) Coordinated remodeling of cellular metabolism during iron deficiency through targeted mRNA degradation. *Cell* 120:99–110.
17. Puig S, Vergara SV, Thiele DJ (2008) Cooperation of two mRNA-binding proteins drives metabolic adaptation to iron deficiency. *Cell Metab* 7:555–564.
18. Zitomer RS, Lowry CV (1992) Regulation of gene expression by oxygen in Saccharomyces cerevisiae. *Microbiol Rev* 56:1–11.
19. Liu Z, Butow RA (2006) Mitochondrial retrograde signaling. *Annu Rev Genet* 40: 159–185.
20. Sánchez E, et al. (2013) LYRM7/MZM1L is a UQCRFS1 chaperone involved in the last steps of mitochondrial complex III assembly in human cells. *Biochim Biophys Acta* 1827:285–293.
21. Cruciat CM, Hell K, Fölsch H, Neupert W, Stuart RA (1999) Bcs1p, an AAA-family member, is a chaperone for the assembly of the cytochrome bc(1) complex. *EMBO J* 18:5226–5233.
22. Denke E, et al. (1998) Alteration of the midpoint potential and catalytic activity of the rieske iron-sulfur protein by changes of amino acids forming hydrogen bonds to the iron-sulfur cluster. *J Biol Chem* 273:9085–9093.
23. Ihrig J, et al. (2010) Iron regulation through the back door: Iron-dependent metabolite levels contribute to transcriptional adaptation to iron deprivation in Saccharomyces cerevisiae. *Eukaryot Cell* 9:460–471.
24. Diaz F, Enríquez JA, Moraes CT (2012) Cells lacking Rieske iron-sulfur protein have a reactive oxygen species-associated decrease in respiratory complexes I and IV. *Mol Cell Biol* 32:415–429.
25. Mimaki M, Wang X, McKenzie M, Thorburn DR, Ryan MT (2012) Understanding mitochondrial complex I assembly in health and disease. *Biochim Biophys Acta* 1817: 851–862.
26. Nishikimi M, Hosokawa Y, Toda H, Suzuki H, Ozawa T (1990) The primary structure of human Rieske iron-sulfur protein of mitochondrial cytochrome bc1 complex deduced from cDNA analysis. *Biochem Int* 20:155–160.
27. Atkinson A, et al. (2011) The LYR protein Mzm1 functions in the insertion of the Rieske Fe/S protein in yeast mitochondria. *Mol Cell Biol* 31:3988–3996.
28. Ferreira M, et al. (2011) Progressive cavitating leukoencephalopathy associated with respiratory chain complex I deficiency and a novel mutation in NDUFS1. *Neurogenetics* 12:9–17.
29. Lopez-Fabuel I, et al. (2016) Complex I assembly into supercomplexes determines differential mitochondrial ROS production in neurons and astrocytes. *Proc Natl Acad Sci USA* 113:13063–13068.
30. Jang S, et al. (2017) Elucidating mitochondrial electron transport chain supercomplexes in the heart during ischemia-reperfusion. *Antioxid Redox Signal* 27:57–69.
31. Winge DR (2012) Sealing the mitochondrial respirasome. *Mol Cell Biol* 32:2647–2652.
32. Moreno-Lastres D, et al. (2012) Mitochondrial complex I plays an essential role in human respirasome assembly. *Cell Metab* 15:324–335.
33. Lu M, et al. (2008) Role of the malate-aspartate shuttle on the metabolic response to myocardial ischemia. *J Theor Biol* 254:466–475.
34. Genova ML, Lenaz G (2015) The interplay between respiratory supercomplexes and ROS in aging. *Antioxid Redox Signal* 23:208–238.
35. Maranzana E, Barbero G, Falasca AI, Lenaz G, Genova ML (2013) Mitochondrial respiratory supercomplex association limits production of reactive oxygen species from complex I. *Antioxid Redox Signal* 19:1469–1480.
36. Shakoury-Elizeh M, et al. (2010) Metabolic response to iron deficiency in Saccharomyces cerevisiae. *J Biol Chem* 285:14823–14833.
37. Sanvisens N, Bañó MC, Huang M, Puig S (2011) Regulation of ribonucleotide reductase in response to iron deficiency. *Mol Cell* 44:759–769.